Tellus
SERIES A
DYNAMIC
METEOROLOGY
AND OCEANOGRAPHY
PUBLISHED BY THE INTERNATIONAL METEOROLOGICAL INSTITUTE IN STOCKHOLM

Tellus (2008), 60A, 1023–1037
Printed in Singapore. All rights reserved

TELLUS

Evaluation of European Land Data Assimilation System (ELDAS) products using in situ observations

By C. M. J. JACOBS[1,*], E. J. MOORS[1], H. W. TER MAAT[1], A. J. TEULING[2], G. BALSAMO[3,4], K. BERGAOUI[3], J. ETTEMA[4,5], M. LANGE[6], B. J. J. M. VAN DEN HURK[7], P. VITERBO[4,8] and W. WERGEN[6], [1]*Alterra, Wageningen UR, Droevendaalsesteeg 4, P.O. Box 47, 6700 AA Wageningen, The Netherlands;* [2]*Wageningen University, Hydrology and Quantitative Water Management Group, Wageningen, The Netherlands;* [3]*Météo-France-CNRM, Toulouse, France;* [4]*European Centre for Medium-Range Weather Forecasts, Reading, U.K.;* [5]*Utrecht University, Institute for Marine and Atmospheric Research, Utrecht, The Netherlands;* [6]*Deutscher Wetterdienst, Offenbach, Germany;* [7]*Royal Netherlands Meteorological Institute, De Bilt, The Netherlands;* [8]*Instituto de Meteorologia, Lisboa, Portugal*

(Manuscript received 28 June 2007; in final form 5 June 2008)

ABSTRACT

Three land-surface models with land-data assimilation scheme (DA) were evaluated for one growing season using in situ observations obtained across Europe. To avoid drifts in the land-surface state in the models, soil moisture corrections are derived from errors in screen-level atmospheric quantities. With the in situ data it is assessed whether these land-surface schemes produce adequate results regarding the annual range of the soil water content, the monthly mean soil moisture content in the root zone and evaporative fraction (the ratio of evapotranspiration to energy available at the surface). DA considerably reduced bias in net precipitation, while slightly reducing RMSE as well. Evaporative fraction was improved in dry conditions but was hardly affected in moist conditions. The amplitude of soil moisture variations tended to be underestimated. The impact of improved land-surface properties like Leaf Area Index, water holding capacity and rooting depth may be as large as corrections of the DA systems. Because soil moisture memorizes errors in the hydrological cycle of the models, DA will remain necessary in forecast mode. Model improvements should be balanced against improvements of DA per se. Model bias appearing from persistent analysis increments arising from DA systems should be addressed by model improvements.

1. Introduction

Soil moisture is a crucial state variable in Numerical Weather Prediction (NWP) models with a realistic Land Surface Model (LSM). It controls to a large extent the partitioning of energy available at the surface between sensible and latent heat fluxes, and therefore the daily development of the atmospheric boundary layer (Ek and Holtslag, 2004; Santanello et al., 2005). However, typical timescales of moisture changes in the upper metre of the soil are much longer, several weeks to months, than that of changes in tropospheric humidity, hours to days. Thus, soil moisture memorizes model errors in the hydrological cycle. Precipitation forecasts in particular have been shown to be difficult to improve (Ebert et al., 2003). Since the roots are usually modelled to extract water from the upper soil, incorrect initialization of soil moisture in NWP models may therefore result in systematic drift in the soil wetness state (Viterbo, 1996) and hence lead to poor model forecasts (Rhodin et al., 1999).

The drift in soil moisture often results in bias in evapotranspiration. This is highlighted in Fig. 1, that shows observed and modelled cumulative evapotranspiration for two contrasting sites during one growing season in Europe. The model results have been obtained with the Tiled ECMWF Scheme for Surface Exchanges over Land (Van Den Hurk et al., 2000), a state-of-the-art LSM applied in NWP at the European Centre for Medium-Range Weather Forecasts. More details will be given later. The Hyytiälä site (upper panel) is a Finnish site with generally moist conditions. Here, the evapotranspiration is overestimated. The El Saler site (lower panel) is a Spanish site with much drier conditions. Here, the evapotranspiration is systematically underestimated. The example suggests that the systematic errors in evapotranspiration depend on climatological conditions.

At present, the complexity of the NWP systems precludes physically sound and yet feasible solutions to avoid the drift of

*Corresponding author.
e-mail: cor.jacobs@wur.nl
DOI: 10.1111/j.1600-0870.2008.00351.x

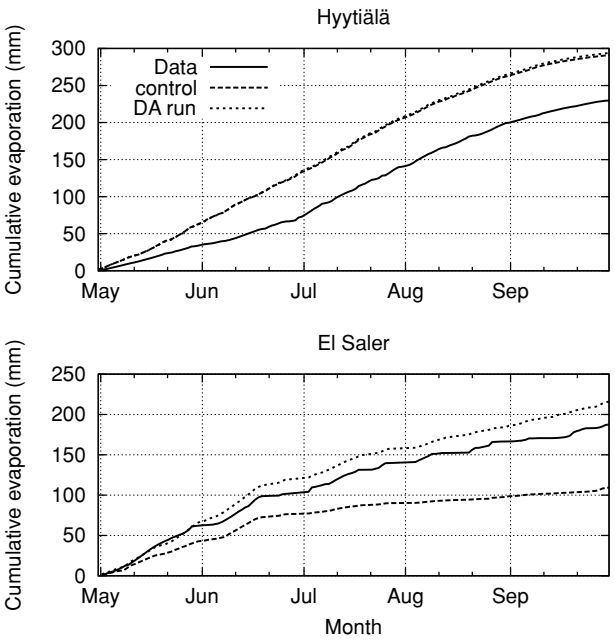

Fig. 1. Illustration of the bias in the cumulative evaporation of the LSM TESSEL and the impact of the data assimilation system. Results are shown from simulations for two climatologically contrasting sites in Europe, during one growing season. The model output is compared with data from eddy covariance measurements. Upper panel: results for Hyytiälä in Finland, representing moist and cool conditions; Lower panel: results for El Saler in Spain, representing dry and warm conditions. See Sections 2 and 3 for more information on the model runs and the data, respectively.

soil moisture and related biases in the models. Soil moisture data assimilation (DA) is regarded as a pragmatic solution to repair biases in land–atmosphere interaction models related to soil wetness state (Van den Hurk et al., 2008). In meteorological applications, the technique has been applied routinely since the mid-nineties (Mahfouf, 1991; Van Den Hurk et al., 1997; Houser et al., 1998; Douville et al., 2000; Hess, 2001; Balsamo et al., 2004). The effects of such systems depend on climatic conditions as well. This is also illustrated in Fig. 1, which depicts results from application of DA (to be detailed later). Considerable improvement is obtained in the dry Spanish climate case (El Saler) but there is hardly any impact in the moist Finnish climate case (Hyytiälä).

Various DA approaches can be followed in order to avoid long-term soil moisture drift. Direct observation and analysis of soil moisture is most tightly linked to the variable of interest but such observations are not routinely available at sufficient spatial resolution. Microwave remote sensing data are increasingly used (Houser et al., 1998; Seuffert et al., 2004) but only reflect the soil state in a very shallow layer. A widespread pragmatic approach utilizes screen-level temperature and humidity (Viterbo, 1996; Hess, 2001). The advantage is that these observations reflect to some extent the atmospheric response to soil moisture, which is desirable in an operational meteorological context (e.g. Mahfouf, 1991). However, the penalty to be paid is that inconsistencies in the modelled energy and water balance are introduced. Model deficiencies may be obscured, which may slow down model improvement.

Evaluation of the current operational land DA systems by comparison of the different systems among each other and with data is crucial in the assessment of the benefits or disadvantages of the DA approach. Comparison experiments like the Atmospheric Model Intercomparison Project (AMIP, see e.g. Robock et al., 1998) have gained considerable insights in the quality and ways of possible improvements of the participating models. Such a comparison is carried out in steps and starts with a confrontation of model results with observations. The results may then inspire further, more detailed analyses carried out to expose the processes and the interactions leading to differences and errors.

Here, we use land DA as a framework to evaluate the soil moisture, surface fluxes and their interaction from three operational meteorological forecast systems by confrontation with observations. The primary goal is to highlight systematic model errors, the impact of modelling assumptions and the effect of DA on the final results. Detailed diagnostics on the reasons for various shortcomings of the modelling systems involved require in-depth knowledge of the physical parametrizations and DA systems. They are beyond the scope of the present paper, but are being performed by the participating forecasting centres (e.g. Van Den Hurk et al., 2008; Hess et al., 2008).

In the context of the project Development of a European Land Data Assimilation System to predict Floods and Droughts (ELDAS; Van Den Hurk, 2002) three operational LSM with DA systems were run for one European growing season (the year 2000). They all have different LSM incorporated in operational NWP models: Interactions between the Soil, Biosphere and Atmosphere (ISBA, Noilhan and Mahfouf, 1996), TERRA (Doms et al., 2005) and Tiled ECMWF Scheme for Surface Exchanges over Land (TESSEL, Van Den Hurk et al., 2000). Also, the basic configuration of the systems was different, stressing the focus of an evaluation under conditions to which the LSM are routinely exposed. Key-features of the LSM and DA systems relevant to the present evaluation study will be outlined in Section 2.

The LSM with their DA systems are evaluated using in situ observations from 33 locations in Europe. The evaluation data originate from various databases that are briefly described in Section 3. The information content of these datasets varies widely among the locations, necessarily implying a different evaluation focus for the respective datasets. To this end, three main topics were selected.

Soil moisture, the quantity that is directly affected by the ELDAS system, was selected as the first focus. Direct observations of soil moisture are only available at a limited number of sites. Therefore, as a second focus the behaviour of net precipitation was chosen. This quantity is defined as gross precipitation (P)

minus evapotranspiration (E). For the evaluation period selected (May–October 2000) and on the timescale of a month, trends in P–E may in most cases be considered as a major driver of trends in soil moisture storage, allowing the use of P–E as a first-order proxy of such trends. The third focus was chosen to be the energy partitioning at the surface, because the soil moisture DA systems considered here are designed to yield a correct energy partitioning in the meteorological models.

The results of the evaluation for the three main topics are presented and discussed in Section 4. Finally, Section 5 contains a discussion and conclusions.

2. Key features of the models and setup of the data assimilation experiment

2.1. General

An overview of the LSM and the main layout of the DA experiment within ELDAS are given in Table 1. A full description of the physics of the LSM can be found in the cited literature. Here, only some key features of the DA experiment and characteristics that are crucial in the interpretation of the results are given.

The present evaluation study is restricted to the period May–October 2000, for which output from all models was available. The models were initiated with the initial state from the operational NWP models on 1 October 1999 for ISBA and TESSEL, and 15 April 2000 for TERRA, respectively. ISBA and TERRA were run in the context of the three-dimensional NWP systems. ISBA was run in the ARPEGE global model (Courtier et al., 1991), which has a Gaussian varying grid size ranging between 17 and 25 km over the ELDAS domain (Balsamo et al., 2005). TERRA is run in the Lokal-Modell (LM; Doms and Schättler, 2002) at a horizontal resolution of 7 km. The model output from ISBA-ARPEGE and TERRA-LM was post-processed to be projected on the ELDAS grid ('nearest neighbour'). The ELDAS grid extended from [35° N, 15° W] to [72° N, 38° E], with a horizontal resolution of 0.2×0.2 degrees. By contrast, TESSEL was run in a single-column (one-dimensional) mode (TESSEL-SCM) in which advection is prescribed as a lateral boundary condition to compensate for the lack of three-dimensional feedback (Van Den Hurk et al., 2008). The horizontal advection terms are derived from re-analysed meteorological fields (ERA-40, Uppala et al., 2005). TESSEL-SCM was run specifically for grid points corresponding to the 33 evaluation sites.

Table 1. Summary of the setup of the ELDAS DA experiment

NWP centre	LSM	Land-surface database	Forcings (P, SW, LW)	Soil moisture assimilation
CNRM	ISBA	Ecoclimap	Model	T, RH, (ELDAS P)
DWD	TERRA	Ecoclimap	Model	T
ECMWF	TESSEL	GLCC	ELDAS	T, RH

Notes: The table lists the NWP partners in ELDAS with their Land Surface Model (LSM), the corresponding database used to describe the land surface (GLCC is the Global Land Cover Characterization; Loveland et al., 2000), the source of the LSM forcings precipitation (P), short-wave radiation (SW), and long-wave radiation (LW), and the screen-level observations used in the DA systems (T is temperature and RH is relative humidity).

ISBA and TERRA construct their land-surface properties from the Ecoclimap database (Masson et al., 2003), while TESSEL utilizes the Global Land Cover Characterization (GLCC, Loveland et al., 2000). For the forcings of the land-surface part, ISBA and TERRA relied on their model-derived precipitation (P), shortwave and long-wave radiation (SW and LW, respectively). TESSEL used the special ELDAS forcing databases for the precipitation (Rubel et al., 2005) and radiation fields (Meetschen et al., 2004), respectively. In the case of ISBA, a correction to soil moisture was applied to account for the difference between model precipitation and ELDAS precipitation forcing (Balsamo et al., 2005).

All DA systems diagnose deviations in the soil moisture fields from forecast errors in screen-level observations. ISBA and TESSEL used temperature (T) as well as relative humidity (RH), but TERRA used T only. Since the soil moisture adjustments are diagnosed from near-surface atmospheric quantities, the formulation of the evapotranspiration, its dependence on soil moisture and the parameters determining the soil moisture evolution are of particular interest. These will be discussed in more detail next.

2.2. Description of evapotranspiration in the models

All models compute the turbulent fluxes using the well-known resistance analogue. For evapotranspiration,

$$E = c_{\mathrm{veg}} \frac{\Delta\rho_{\mathrm{v}}}{r_{\mathrm{a}} + r_{\mathrm{s}}} \ (\mathrm{kg\,m^{-2}\,s^{-1}}), \tag{1}$$

where c_{veg} (−) is some measure of the vegetation cover, $\Delta\rho_{\mathrm{v}}$ (kg m^{-3}) is the difference in water vapour density between the effective source height of water vapour and a reference level in the air, and r_{a} (s m^{-1}) and r_{s} (s m^{-1}) are the aerodynamic and surface resistance, respectively. In the present context, r_{s} is of special interest, because it incorporates the connection between soil moisture and the conditions at the screen level. For vegetation,

$$r_{\mathrm{s}} = \frac{r_{\mathrm{s,min}}}{LAI} \prod_{i=1}^{n} f^{-1}(x_i), \tag{2}$$

where $r_{\mathrm{s,min}}$ (s m^{-1}) is the minimum stomatal resistance under optimal conditions, LAI (m^2 m^{-2}) is the leaf area index and $f(x_i)$ are dimensionless empirical functions to account for effects of environmental conditions on stomatal aperture (Jarvis, 1976). Differences in r_{s} implied by differences in $f(x_i)$ will cause the main difference in the behaviour of the modelled E. The function

$f(\theta)$ describing the impact of soil moisture on r_s determines the sensitivity of screen level parameters to soil moisture conditions (Mahfouf, 1991). The impact of the DA schemes on evapotranspiration will therefore be sensitive to $f(\theta)$.

2.3. Coupling between soil moisture, evapotranspiration and screen level observations

The link between the screen level observations and soil moisture is provided by evaporative fraction, Λ, defined as

$$\Lambda \equiv \frac{\lambda E}{H + \lambda E} \tag{3}$$

where H (W m^{-2}) is the sensible heat flux and λ (J kg^{-1}) is the latent heat of vaporization. This link can be further examined by rewriting the sensitivity equation for λE to r_s given by Jacobs and De Bruin (1992) as:

$$\frac{\partial \Lambda}{\partial r_s} = \frac{-\Lambda}{(1 + s/\gamma) r_a + r_s} \tag{4}$$

which can readily be derived from the well-known Penman–Monteith equation. Here, s (kg kg^{-1}K^{-1}) is the slope of the saturation specific humidity versus temperature curve and γ (K^{-1}) $\equiv c_p/\lambda$ is the psychrometric constant, where c_p (J kg^{-1} K^{-1}) is the specific heat capacity of the air. Equation (4) represents the change in Λ per unit change in r_s. In the models considered here, the response of r_s to soil moisture is modelled using in (2):

$$f(\theta) = \begin{cases} 0 & \theta < \theta_w \\ \frac{\theta - \theta_w}{\theta_c - \theta_w} & \theta_w \le \theta < \theta_c \\ 1 & \theta \ge \theta_c \end{cases} \tag{5}$$

where θ_w (m^3 m^{-3}) is the wilting point and θ_c (m^3 m^{-3}) a critical moisture content defining the transition between supply and demand limited transpiration. ISBA and TESSEL assume θ_c to be equal to the field capacity θ_{fc} [kg m^{-3}], by which the second member of (5) becomes equal to the Soil Water Index. In TERRA θ_c is the so-called turgor loss point which is computed dynamically as a function of the water holding capacity and the potential evaporation, following Denmead and Shaw (1962). By virtue of (5), r_s and Λ are sensitive to θ only in the range $\theta_w \le \theta < \theta_c$. Because of absence of synergy in (2), the modelled sensitivity of r_s to θ in this interval can to first order be written:

$$\frac{\partial r_s}{\partial \theta} = \frac{-r_s}{\theta - \theta_w} \tag{6}$$

so that

$$\frac{\partial \Lambda}{\partial \theta} = \frac{\Lambda}{\theta - \theta_w}(1 - \Omega) \tag{7}$$

with

$$\Omega \equiv \left[1 + \frac{\gamma}{s + \gamma}\frac{r_s}{r_a}\right]^{-1} \tag{8}$$

where Ω is the decoupling factor (Jarvis and McNaughton, 1986), describing to what extent the surface and the conditions at a reference level are coupled. It attains values between 0 and 1 and is mainly influenced by the surface characteristics implicit in r_s and r_a. It is further modulated by temperature, through the dependence of s on temperature.

Equation (7) provides a justification of DA approaches where forecast errors in screen level observations are used to diagnose soil moisture deviations and to improve the energy partitioning by adjusting the soil moisture. The required sensitivity is present in the models by virtue of stress function (5). Apart from the somewhat intuitive result that Λ should decrease with decreasing soil moisture, eq. (7) shows that the impact of soil moisture changes on Λ is expected to be largest for well-coupled surfaces such as forests (high r_s, low r_a). The sensitivity is strongly enhanced by dry soils in two ways: (1) by decreasing the soil moisture content which reduces $\theta - \theta_w$; (2) by increasing r_s and therefore $(1 - \Omega)$. Thus, eq. (7) implies that a given soil moisture increment will have a larger impact on Λ in dry conditions than in wet conditions. Although the sensitivity will be modulated by feedback with the Atmospheric Boundary Layer (Jacobs and De Bruin, 1992; Ek and Holtslag, 2004) this equation may support interpretation of the main differences in the impact of the various DA systems on Λ.

2.4. Water holding capacity

Soil moisture is a relatively slowly varying variable. Of paramount importance is the water-holding capacity, defined here as the difference between field capacity and wilting point for a soil layer with depth 1 m. The water holding capacity depends on soil texture and differs considerably among the models, as shown in Table 2. The largest range in water holding capacity per unit soil depth is modelled in TERRA. Although ISBA computes wilting point and field capacity from the textural composition of the soils, the actual range of water holding capacity ($\sim$80 mm) is small. TESSEL uses one uniform soil type. The minimum sensitivity of Λ to soil moisture content is directly controlled by the water holding capacity, as can be seen from (7): the minimum sensitivity is obtained as $\theta \to \theta_{fc}$. Note that then $f^{-1}(x_n) \to 1$. For otherwise similar conditions the sensitivity is inversely proportional to the water holding capacity. Thus,

Table 2. Water holding capacity (mm) for different soil types in ISBA, TERRA and TESSEL

Soil	ISBA	TERRA	TESSEL
Sand	73	154	152
Sandy loam	82	160	
Loam	88	230	
Loamy clay	89	185	
Clay	85	206	

Note: Here, water holding capacity is defined as the difference between field capacity and wilting point for a 1–m deep layer of soil.

under well-watered conditions and for similar rooting depth, the sensitivity of Λ in ISBA may be expected to be roughly twice that of TESSEL, and up to three times that of TERRA.

The amount of water available for evapotranspiration is both a function of the water holding capacity as defined in Table 2 and of rooting depth. The latter characteristic also differs among the models. TERRA utilizes an empirical temporal variation of rooting depth. For the period, locations and vegetation types considered here, rooting depth in TERRA typically varies from 20–50 cm in May, with a maximum of 60–70 cm in July and August and then decreasing to 10–20 cm in October again. ISBA uses a fixed rooting depth between about 1 and 2 m, depending on the vegetation and location. TESSEL prescribes a root density that decreases exponentially with depth, again depending on the vegetation. For the vegetation considered here, about 90% of the roots are located in the upper metre of the soil, with about 30% of the roots being located in the upper model layer of 0.07 m. TESSEL accounts for the preference of roots to extract water from relatively wet layers (Van den Hurk et al., 2000).

In conclusion, while vegetation in ISBA and TESSEL utilizes the moisture available in the upper first metre of the soil, TERRA only uses part of the available moisture. However, in TERRA a seasonal dependence is modelled.

3. In situ observations and evaluation methodology

3.1. General

As outlined above, the DA is expected to affect various components in the surface water and energy balance. Here we use observations to address three aspects in particular:

1. How well do the ELDAS systems reproduce the temporal dynamics of the soil moisture content? This is diagnosed by comparing the ELDAS products to observed changes in soil moisture derived from a set of in situ observations.
2. Do the DA increments improve the soil water balance on a monthly scale? Observations of precipitation and evaporation are used to estimate changes in the soil water volume, and to relate the magnitude of the DA increments to the other water balance terms.
3. Do the soil moisture adjustments in the DA systems improve the partitioning of available energy over sensible and latent heat flux? Here, modelled and observed evaporative fraction are compared.

Figure 2 shows the locations of the 33 sites where observational data used in the present evaluation study were collected. The observations were performed in the context of different field campaigns, set up with different purposes. Therefore, the information content of the data sets varies widely among the locations. Also, a large range of climatic conditions is represented in the data.

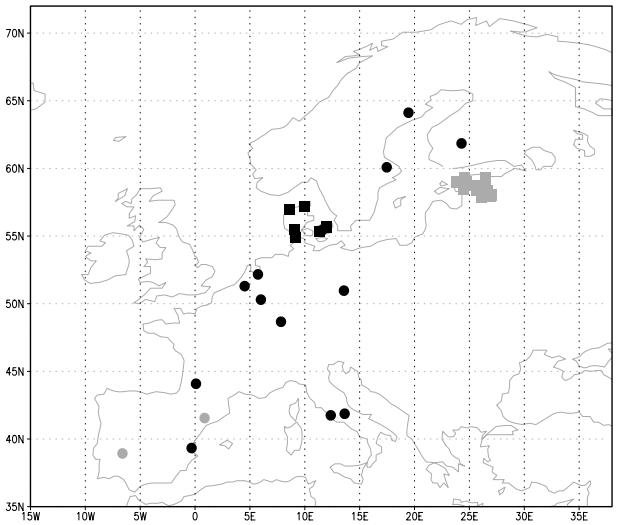

Fig. 2. Location of the ELDAS evaluation sites. Black circles: CarboEurope sites; Grey circles: Scintillometer sites; Black squares: PLAP sites; Grey squares: BALTEX sites. See text for a further description of the sites.

At 24 out of the 33 evaluation sites, direct soil moisture observations were performed. These sites are henceforth called 'soil moisture sites'. Some of the soil moisture observations show great detail in space and time. At all soil moisture sites precipitation is measured. Occasionally, other observations such as soil temperature are available, but at most of the soil moisture sites turbulent fluxes of latent and sensible heat were not observed.

At 14 out of the 33 sites micrometeorological observations of the turbulent fluxes were performed. These sites will be referred to as 'flux sites'. The flux measurements were generally accompanied by observations of meteorological variables such as temperature, humidity and radiation. At the majority of the sites, precipitation was observed as well. However, soil moisture was measured at a limited number of the flux sites only.

3.2. Data sources

3.2.1. The Danish Pesticide Leaching Assessment Programme (PLAP). This programme was designed to monitor the leaching behaviour of pesticides or their degradation products to groundwater. At six PLAP monitoring sites detailed observations of soil moisture and temperature profiles were performed. The observations in the soil were accompanied by observations of precipitation. For a detailed description of the sites and the measurements the reader is referred to (Lindhardt et al., 2001).

3.2.2. BALTEX-Estonia. The Baltic Sea Experiment (BALTEX) is an international research initiative aimed at understanding the hydrological balance and energy exchange of the Baltic sea drainage basin (Raschke et al., 2001). For the ELDAS evaluation period, soil moisture content and precipitation data were made available for the Estonian region.

3.2.3. CarboEuroflux. The major goal of the CarboEuroflux program is to improve the understanding of the magnitude and temporal and spatial variability of the carbon source and sink strengths of terrestrial ecosystems (Valentini et al., 2000). The main data available from these sites are Eddy Covariance (EC) observations of the turbulent fluxes, obtained following prescribed experiment and data processing protocols (Aubinet et al., 2000). For the ELDAS year 2000, observations of H and λE were available at 13 forested sites, distributed over the European continent. Precipitation was observed at all but one of the CarboEuroflux sites used here. At some sites, soil moisture content was observed at depths below 20 cm and seasonal trends derived from these observations were included in the present analysis.

3.2.4. Scintillometer observations in Spain. For one site in Spain, flux observations were available from the large scale Energy and Water Balance Monitoring System project (EWBMS; Moene and De Bruin, 2001). These measurements were performed with a Large Aperture Scintillometer (LAS), in an irrigated area near Badajoz in Spain. LAS can be used to measure sensible heat flux H over distances of 5–10 km and can even be applied to determine average fluxes over the various surface types within the scintillometer path (Meijninger et al., 2002). However, because the LAS only measures H directly, λE has to be derived from the surface energy balance:

$$\lambda E = Q_* - G - H, \tag{9}$$

where Q_* (W m^{-2}) is the net radiation and G (W m^{-2}) is the soil heat flux. Observations of precipitation and the amount of irrigation in the scintillometer area were also available.

3.3. Data processing

In accordance with the differing information content of the evaluation datasets, three main evaluation topics were chosen.

3.3.1. Soil moisture. In order to avoid disparities due to the different discretization of the models, the moisture content in the upper metre of the soil [$\theta_{1\mathrm{m}} \equiv \int_0^1 \theta(z)\mathrm{d}z$] was considered. This layer is also representative for the most relevant (seasonal) timescale of soil moisture variations in the NWP context (Viterbo and Beljaars, 1995). The water utilized for evapotranspiration is generally extracted from this layer as well. At some evaluation sites $\theta_{1\mathrm{m}}$ was observed directly. Analysis of detailed data from these sites showed that $\theta_{1\mathrm{m}}$ and observed soil moisture content at specific levels below 20 cm follow similar trends. Therefore, such observations are used to approximate the trend in $\theta_{1\mathrm{m}}$ for locations where direct observations of $\theta_{1\mathrm{m}}$ were not available.

Due to the large spatial variability of soil moisture, in situ soil moisture observations generally differ from larger scale estimates such as those made at the LSM grid size. However, for the atmosphere the relevant land surface variable is the amount of water returned to the atmosphere by evapotranspiration. Here, the corresponding storage change is expressed in terms of a soil moisture change relative to a reference value. To avoid difficulties in defining an adequate reference soil moisture content from the soil hydraulic properties, it was decided to express $\theta_{1\mathrm{m}}$ changes relative to the 95-percentile value $\theta_{1\mathrm{m}}^{95}$ of the evaluation period at the sites. Over the period considered here, about nine extreme daily values are then disregarded, so that the analysis becomes insensitive to outliers. In addition, the seasonal amplitude of the soil water storage is expressed as the difference between $\theta_{1\mathrm{m}}^{95}$ and the 5-percentile value $\theta_{1\mathrm{m}}^{5}$.

3.3.2. Net precipitation, P–E. Although our DA systems are designed to optimize evapotranspiration, it is implicitly assumed that the soil moisture increments improve the seasonal cycle of the soil water balance:

$$\Delta W = P - E + \delta W - (R + D), \tag{10}$$

where W is the bulk soil moisture content, δW denotes the increments from the DA system, R is runoff and D is drainage. For the observations δW is zero. Runoff and drainage are not observed at the sites considered.

To first order, net precipitation P–E is an indicator of soil moisture storage changes if runoff and drainage are relatively small loss terms in (10). On the timescale and in the period considered here, gross precipitation (P) is the major input of soil moisture, while evapotranspiration (E) represents the major output at most evaluation sites. The effect of the DA system can therefore be assessed by comparing P–E from the observations with $P - E + \delta W$ and P–E, respectively, from the models. Because this analysis requires E, it can only be performed for flux sites.

The condition of low runoff and drainage rates was checked for all three models over the period considered here. For ISBA $(R + D)$ was less then 15% of P at 30 out of the 33 evaluation sites, with an average of 5%. For TERRA, $(R+D)$ was less than 15% of P in 31 out of 33 cases, with an average of 7%. Thus, in these cases on average more than 90% of the soil moisture storage changes are driven by changes in $(P-E)$ or $(P - E + \delta W)$, respectively. The modelled $(R + D)$ was typically between 20% and 40% of P in the case of TESSEL, with 8 out of 33 cases having smaller contributions and 2 out of 33 cases having larger contributions from $(R + D)$. The mean fraction was 27%, implying that on average still about three-quarters of the changes in soil moisture storage are driven by $(P-E)$. However, in individual cases the $(P-E)$ estimate may not be representative for the storage change. In such cases the impact of the DA system can still be assessed when the difference in $(R + D)$ with and without DA system is much smaller than δW. This second condition could be checked for the TESSEL simulations, because for this model control simulations were available. We performed such a check for five flux sites where $(R + D) > 0.3P$. In three cases the change in $(R + D)$ was clearly less than δW, while in two cases $(R + D)$ was similar to δW.

From this analysis we conclude that in our case the effect of the DA systems on soil moisture storage can be evaluated by comparing $(P - E + \delta W)$ with $(P - E)$. However, because the uncertainty is typically some 5–10% on average, the results, notably those of individual sites, should be interpreted with care. In a few individual cases where the effect of $(R + D)$ on soil moisture storage is comparable to the one of $(P - E + \delta W)$, the methodology is just indicative of the effect of the DA system on the *meteorological drivers* of soil moisture, and not of soil moisture itself.

Cumulative values of P, E and δW over periods of one month are considered for the flux sites. This time scale corresponds to typical timescales of moisture changes in the upper metre of the soil. Observed P was taken from the ELDAS precipitation database (Rubel et al., 2005). This database consists of three-hourly precipitation sums for each grid point in the ELDAS domain, constructed from over 20 000 rain gauge observations and radar observations in Europe. This data source is preferred over the local observations, because it guarantees high-quality observations of P to be available for all sites, at all times in the evaluation period. Furthermore, it matches the spatial scale of the model resolution, and the quality of the ELDAS precipitation database is probably best in the period that is considered here (Rubel et al., 2005).

3.3.3. Evaporative fraction, Λ. The third major focus of the present evaluation study was chosen to be Λ, defined by (3). It is an important diagnostic in land-surface schemes (Ek and Holtslag, 2004; Betts and Viterbo, 2005), and may also serve as a soil-moisture indicator (Bastiaanssen, 1995). Λ quantifies the partitioning of available energy between heating and moistening the Atmospheric Boundary Layer (ABL). It controls to a large extent the ABL dynamics, including the formation of clouds within the ABL (Ek and Holtslag, 2004; Betts and Viterbo, 2005). Because it is a normalized flux, Λ allows a fair comparison between the model and the observations, independent of differences between prescribed and real albedo and radiative forcing.

Obviously, only data from flux sites could be used in this analysis. Data treatment from these sites needed special care in order to ensure meaningful analyses of Λ. Using data from the CarboEuroflux community the basic quality requirements regarding instrument configuration and processing of the data (Aubinet et al., 2000) are met. The remaining uncertainty in the energy fluxes is typically 10–15% for midday values (Mauder et al., 2007). Lack of energy balance closure has often been regarded as a basic flaw of EC measurements (Oncley at al., 2007). However, in a recent study by Jacobs et al. (2008) it was found that for a flat homogeneous surface with good fetch conditions the 'missing energy' is entirely due to non-turbulent terms, such as dew formation, heat storage in soil, vegetation and air, and photosynthesis. This implies that no 'systematic' bias due to lack of energy balance closure exists in the measured 'turbulent' fluxes, as long as the EC data are obtained and processed according to the generally accepted quality guidelines, like those of Aubinet et al. (2000).

The data were post-processed as follows. Daily values of Λ were computed for every flux site ($n = 14$) using only mean hourly values of H and λE between 10 and 15 UTC. For the sites considered here, the selected daytime period contains local noon in all cases. Observations were excluded if precipitation had occurred during the averaging period, and if the observed wind speed was less than 1 m s^{-1}. For both the model and the observations it was also required that $H > -20$ W m^{-2} and $\lambda E > 10$ W m^{-2} (with upward fluxes taken positive). These requirements exclude extremely stable conditions under which Λ is a poor indicator of the surface energy balance partitioning and of soil moisture. Finally, Λ for a specific day was included only if it could be computed from at least four out of five hourly flux values after the aforementioned data screening procedure.

For the period May–September, average monthly differences between modelled and observed Λ were computed for each flux site if in a particular month at least 50% of the noontime differences was available at that site. For each month the mean differences were then averaged over all sites with sufficient data in that month. October was not considered in this analysis because in that month Λ usually plays no meaningful role as a soil moisture indicator anymore. Wet conditions due to precipitation often led to a stably stratified atmosphere in October, so that only a small number of high-quality Λ values could be obtained.

4. Results

4.1. Soil moisture

Figure 3 shows the observed and simulated soil moisture change $\theta_{1\mathrm{m}} - \theta_{1\mathrm{m}}{}^{95}$ of Vielsalm, (Belgium), El Saler (Spain) and Faardrup (Estonia). These cases were selected because they represent climatologically moist and dry locations, respectively. At Vielsalm and El Saler, the observations have been obtained at a depth below 20 cm in the soil, where the soil moisture dynamics were representative of those of $\theta_{1\mathrm{m}}$. In Faardrup, reports of $\theta_{1\mathrm{m}}$ were available.

It can be seen that the models are quite capable of simulating the situation in the moist case of Vielsalm. The amplitude and the timing of the variations in soil moisture are reasonably well simulated, especially from day 175 onwards. In contrast, the soil moisture variations are generally poorly simulated for the dry case of El Saler and Faardrup. In the observations of El Saler, $\theta_{1\mathrm{m}}$ rapidly recovers from precipitation events, while in the models the rapid variations are suppressed. The rainfall event on day of year (DOY) 295 has a clear impact on the output from ISBA and TESSEL. TERRA does not use the observed precipitation, and misses the magnitude of such events in El Saler as well as in Faardrup. Over the whole season, only TERRA captures the range in the observed $\theta_{1\mathrm{m}}$ while the other two

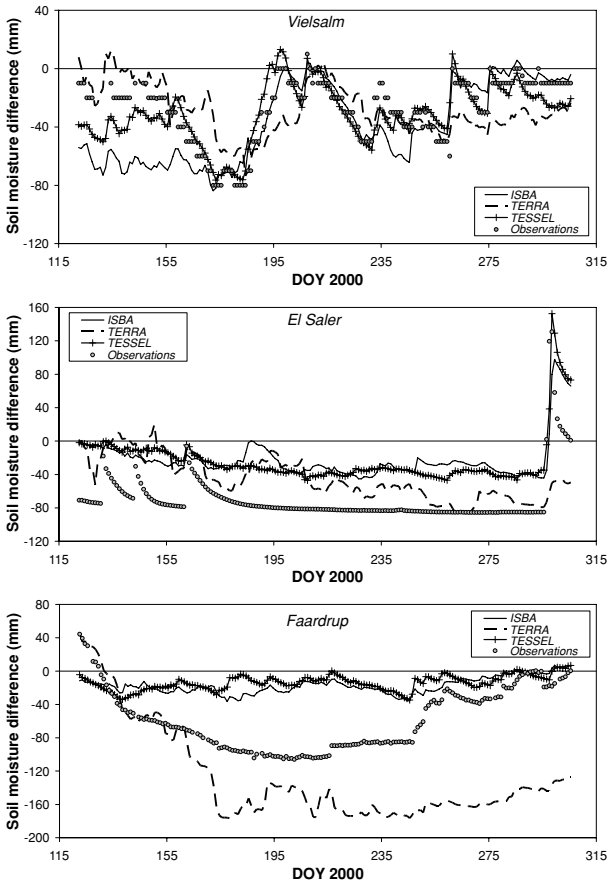

Fig. 3. Modelled and observed soil moisture storage change for the evaluation sites Vielsalm (upper panel), El Saler (middle panel) and Faardrup (lower panel) during the evaluation period. Note the difference in scales. The storage change is computed relative to $\theta_{1\mathrm{m}}^{95}$, the 95-percentile of the observed or computed soil moisture content.

systems remain relatively wet. This is the case in both El Saler and Faardrup.

Analysis of the soil hydrological balance in El Saler, after a rainfall event, suggests that the high values are caused by addition of soil water by the DA system (see below). Indeed, on average, the models overestimate the daytime temperature and underestimate the relative humidity in this period, which drives the addition of water. For example, the average temperature deviation (model – observation) at 12 UTC was 3.9 K for ISBA (range 10.8–0.7 K), 5.7 K for TERRA (range 13.0 to –2.5 K) and 1.6 K for TESSEL (range 8.8 to –11.6 K), while the average deviation of relative humidity amounted to 11% for ISBA (range 46% to −12%), 5% for TERRA (range 32 to −20%) and 11% for TESSEL (range 50% to −32%). Note that TERRA does not use relative humidity to determine the increments (see Table 1). The biases could be related to a too strong entrainment of dry and warm air into the ABL, an underestimation of the evapotranspiration, or mesoscale circulations that induce advection of cooler and more humid air. Full explanation of the temperature and humidity biases would need further detailed analyses, which is beyond the scope of this paper.

Table 3. Components of the soil hydrological balance of the upper metre in the soil at evaluation site El Saler (Spain), given as sums over the period DOY 162–191. P is the precipitation; E is the evapotranspiration; δW represents the increments due to the data assimilation; $\Delta S_{1\mathrm{m}}$ is the storage change of water in the upper 1 m of the soil; 'Other' includes runoff, drainage and changes in water storage of layers below 1 m

	DATA	ISBA	TERRA	TESSEL
P (mm)	2	0	3	0
E (mm)	−41	−116	−107	−69
δW (mm)		122	80	27
$\Delta S_{1\mathrm{m}}$ (mm)		7	−17	−32
Other		1	7	10

Table 3 highlights the El Saler water balance terms in the period between DOY 162 and DOY 191, just after a rainfall event that occurred on DOY 161. On DOY 162, $\theta_{1\mathrm{m}} - \theta_{1\mathrm{m}}{}^{95}$ is about equal for the observations and the models. After that date, the soil dries out because there is hardly any precipitation. For all three schemes, the computed evapotranspiration is too high. However, in the case of ISBA, the output of soil water by evapotranspiration is fully compensated by input of water from the DA scheme and the soil water content increases. For TERRA, the compensation of evapotranspiration by the DA scheme amounts to 75%. This suggests that in these models, the amplitude of θ_{1m} is almost entirely damped by the DA scheme in the case of El Saler. For TESSEL, the compensation of evapotranspiration by the DA scheme is about 40%. However, the evapotranspiration term is overestimated much less than in the case of ISBA and TERRA. As a result, the modelled net loss of water from the soil (42 mm) corresponds quite well with the observed one (39 mm).

The results for ISBA and TESSEL of Faardrup show that underestimation of the seasonal amplitude may also occur under more temperate climatological conditions (Fig. 3). An analysis of the soil hydrological balance was made for this site as well (Table 4), for the period between DOY 137 and 167 during which the observed soil moisture content consistently decreased (see Fig. 3). Note that evapotranspiration data were not available here, but instead, $\theta_{1\mathrm{m}}$ was reported. Again, $\theta_{1\mathrm{m}}$ of the models and from the observations are similar at the start of this particular period. TERRA was able to follow the observed decrease of $\theta_{1\mathrm{m}}$ until ∼DOY 160, while ISBA and TESSEL even simulated an increase of $\theta_{1\mathrm{m}}$. The observed rainfall over the period amounted to 38 mm. The total change in soil moisture storage down to 2.1 m below the surface was about 44 mm, from which we estimate that water loss by evapotranspiration, runoff and drainage was ∼82 mm over those layers. Using the cumulative runoff and drainage from the models (∼15 mm), we estimate an

Table 4. Components of the soil hydrological balance of the upper metre in the soil at evaluation site Faardrup (Estonia), given as sums over the period DOY 137–167. P is the precipitation; E is the evapotranspiration; δW represents the increments due to the data assimilation; $\Delta S_{1\mathrm{m}}$ is the storage change of water in the upper 1 m of the soil; 'Other' includes runoff, drainage and changes in water storage of layers below 1 m

	DATA	ISBA	TERRA	TESSEL
P (mm)	38	63	40	63
E (mm)		−101	−54	−87
δW (mm)		39	−68	39
$\Delta S_{1\mathrm{m}}$ (mm)	−36	9	−82	15
Other		8	0	0

evapotranspiration loss of ∼67 mm. TERRA simulated the amount of precipitation quite closely (41 mm). Evapotranspiration was 54 mm, while the DA system extracted 65 mm of water. As a result, in this case the decrease in soil water storage is ultimately overestimated (after DOY 160). We note that spin-up effects may have affected the TERRA simulations to some extent (see below). By contrast, ISBA and TESSEL overestimated precipitation (63 mm) and most probably evapotranspiration as well (101 mm for ISBA and 87 mm for TESSEL, respectively). Their DA systems added 39 mm of water, which completely compensates the losses. As a result, $\theta_{1\mathrm{m}}$ remains high and even increases somewhat.

Underestimation of the amplitude of $\theta_{1\mathrm{m}}$ due to the addition of water by the DA systems might be an important characteristic of the systems investigated here. Therefore, the modelled and observed seasonal amplitude of $\theta_{1\mathrm{m}}$ was compared for all evaluation sites where a direct or approximated trend of $\theta_{1\mathrm{m}}$ could be calculated (22 sites). The amplitude is computed simply as the difference between the 5% and 95%-percentile values of θ_{1m} in the evaluation period May–October 2000. It contains information on the amplitude of the seasonal cycle as well as on trends at shorter timescales such as induced by precipitation (see the El Saler example discussed above).

Results are depicted in Fig. 4. Amplitudes > 75 mm are quite common in the observed values. TERRA is the only model capable to mimic such amplitudes, with values up to about 170 mm. However, inspection of a number of cases revealed that the timing of the minima and maxima was quite wrong (not shown here). Moreover, modelled amplitudes did not always match observed amplitudes for specific sites (Fig. 3). Amplitudes of ISBA and TESSEL remain below 75 mm for all sites.

4.2. Net precipitation

For the flux sites with direct observations of evapotranspiration (14 sites) observed P–E was computed for all months of the evaluation period (May–October). Figure 5 shows an example of P–E and $P - E + \delta W$ for the evaluation site Flakaliden in Sweden. The cumulative time series are reset monthly to ease the comparison.

The results for this particular site illustrate a couple of quite typical features of the ELDAS systems. Comparing the balance terms with and without δW shows that in some months the DA scheme improves the modelled soil hydrological balance, in others it does not. TESSEL performs rather well over the entire period and the increments improve the performance a little further. This is at least partially explained from the fact that the observed ELDAS P is used directly in TESSEL. In contrast, the DA scheme of TERRA seems to deteriorate the output of this model. While the initial estimate of P–E agrees reasonably well with the observations the results for $P - E + \delta W$ are much worse. This adverse effect of the DA scheme in TERRA was found in a number of other cases as well, and seems to be typical for the first one or two months, not for the third and subsequent months. An analysis of several model diagnostics showed that this is probably an effect of spin-up, as the assimilation was initially started from interpolated fields from a global model that has a free-running soil (Wergen et al., 2005). The output from ISBA is significantly improved by the DA scheme. However, the main improvement is due to the soil moisture correction based on the precipitation bias. The relatively poor estimate of P–E

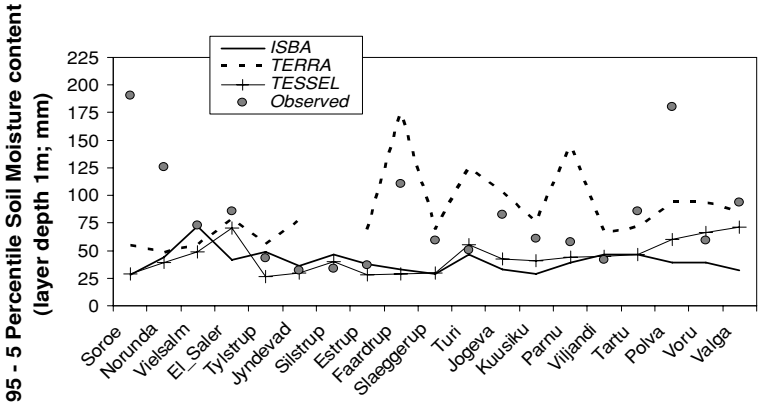

Fig. 4. Comparison of observed and modelled amplitudes of the soil moisture content in the upper metre of the soil. The amplitude is defined as the difference between the 95 and 5 percentile daily values, respectively, in the evaluation period (May–October 2000). Labels on the x-axis denote the evaluation sites. The model outputs are connected by a line to facilitate comparison with the data.

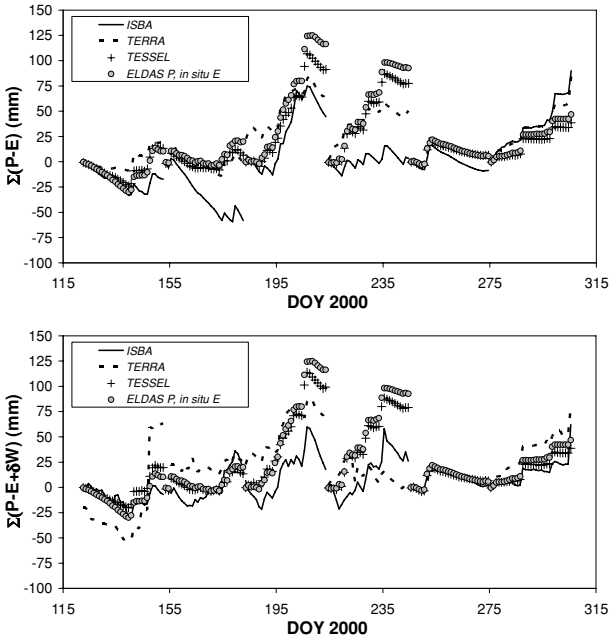

Fig. 5. Illustration of the effect of the data assimilation increments on the soil hydrological balance. Case study Flakaliden (Sweden). Upper: *P–E*; Lower: *P–E* for the data and $P - E + \delta W$ for the models. δW denotes the contribution from the data assimilation. Values shown are cumulative values, reset to zero at the start of each month.

from ISBA was mainly due to the fact that *P* was quite far off in this case (not typical for all sites). These deviations triggered large *P*-related corrections in the ISBA scheme that considerably improved the modelled soil hydrological balance. In some cases, this correction completely cancelled the increments due to the 2D-Var component of the DA scheme in ISBA.

For the flux sites, monthly cumulative observed *P–E* was compared to modelled *P–E* and $P - E + \delta W$, respectively, if the data coverage of observed *E* in a particular month was at least 67% ($n = 13$ for May–June; $n = 12$ for July–October). Mean monthly bias of *P–E* and $P - E + \delta W$ and the root mean square error (RMSE) of the monthly sums from the differences at the evaluation sites were computed. The monthly results are depicted in Fig. 6. The averages over all months in the evaluation

Table 5. Mean monthly bias (model-observations) and RMSE in *P–E* and $P - E + \delta W$, respectively, for ISBA, TERRA and TESSEL, computed for the period May–October 2000

	Bias *P–E* (mm)	Bias $P - E + \delta W$ (mm)	RMSE *P – E* (mm)	RMSE $P - E + \delta W$ (mm)
ISBA	−24.7	−6.0	53.4	44.6
TERRA	−33.6	−5.8	55.5	52.7
TESSEL	−13.1	−0.9	28.1	24.0

period are given in Table 5. A negative bias means that the model is too dry.

It can be seen that including the increments considerably reduced the bias in all models in most months, suggesting a beneficial effect of the DA system on the soil water balance. Only in October the DA system has hardly any effect on the bias in the monthly sums. In the case of TESSEL a gradual systematic decrease of the bias during the growing season can be seen. There is also a reduction of the RMSE, of about 16% for ISBA, 15% for TESSEL and only about 5% for TERRA. This much lower improvement in the case of TERRA is related to the spin-up problems mentioned above and to the use of *P* from the model rather than from observations. The improvement in the case of ISBA is mainly due to the *P*-based correction. The effect on the RMSE is much less systematic than the effect on the bias. Some months show a clear improvement with respect to RMSE, others do not. Again, the largest improvement in the case of TESSEL is obtained in the first part of the evaluation period and gradually decreases towards October.

4.3. Evaporative fraction

The RMSE of Λ on a monthly timescale was computed from the monthly averaged differences per site. The result is shown in Fig. 7 for the individual months and in Table 6 for the seasonal mean. In addition, the role of Λ as a diagnostic of relatively fast dynamic boundary layer processes in NWP models gave rise to the calculation of the RMSE in a particular month from daily

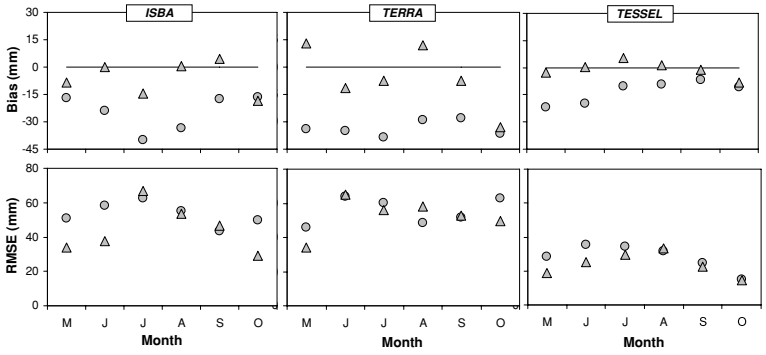

Fig. 6. Bias (model-observations) and RMSE of monthly sums of *P–E* (circles) and $P - E + \delta W$ (triangles) for ISBA (left-hand side), TERRA (middle) and TESSEL (right-hand side), respectively.

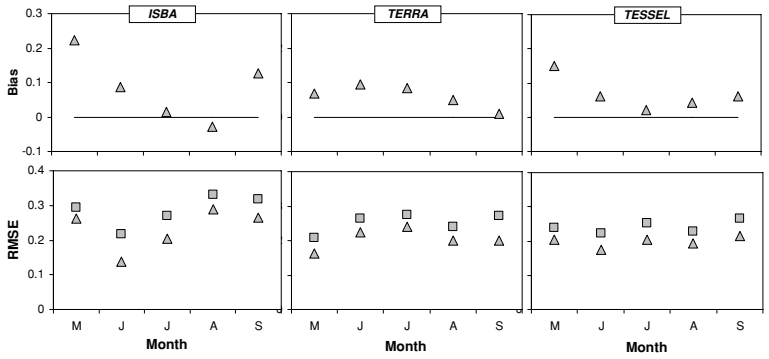

Fig. 7. Bias (model-observations) and RMSE of the evaporative fraction Λ on a monthly timescale (triangles) for ISBA (left-hand side), TERRA (middle) and TESSEL (right-hand side), respectively. Also shown in the lower panels is the RMSE of Λ on a daily timescale (squares).

Table 6. Seasonal mean of bias and RMSE in Λ from errors on a monthly timescale as well as the seasonal RMSE in Λ from errors on a daily timescale. Months included are May–September

	Bias Λ (monthly)	RMSE Λ (monthly)	RMSE Λ (daily)
ISBA	0.085	0.23	0.27
TERRA	0.060	0.21	0.24
TESSEL	0.066	0.20	0.24

errors if at least 15 error estimates were available at the site. The RMSE on this daily timescale, averaged over all sites, is also shown in Fig. 7. Moreover, Table 6 shows the seasonal mean of the RMSE on a daily timescale.

The average bias of the models varies between 0.06 and 0.09. These numbers correspond to 12–17% of the average observed Λ (0.50, range 0.31–0.71). The RMSE varies between 0.20 and 0.23 on the monthly timescale, and between 0.23 and 0.27 on the daily timescale, which corresponds to 40–46% and 46–54% of the average Λ. Because the midday values of Λ show relatively little variation around the monthly mean, the errors at the monthly and daily timescale are correlated. During the evaluation period, a seasonal cycle can be observed in the bias, but not in the RMSE. The trend in the bias is similar for ISBA and TESSEL, with minimum deviations in July–August. TERRA shows a reversed trend with a maximum deviation in June–July. Even with DA system, the bias is considerable. Because of the tendency of the models to keep the soils wet (see above), the link between the screen-level observations and soil moisture, and the impact of the DA systems on Λ is weak.

The influence of the DA system on the quality of Λ cannot be evaluated from the information given above. Only in the case of TESSEL a control run without DA was performed. A limited screening of the effect was performed for this model by comparing the output from the control run and the DA run in a dry and a moist situation (see Van Den Hurk et al. (2008) for a more extensive discussion of the increments). The differences between dry and moist conditions should lead to quite different impacts of the DA systems (see Section 2.3). Figure 8 shows the 11-d moving average of the noontime Λ for El Saler (Spain, dry case) and Soroe (Denmark, wet case), respectively. It can be seen that after the first few weeks in the case of El Saler Λ is too small in the control run. In the DA run Λ becomes too high. The overcorrection may be due in part to the high sensitivity of Λ to soil moisture under dry conditions. As was shown in Section 2.3, such high sensitivity is implicit in all the models because of the characteristics of the functions that account for root water extraction. By contrast, in the case of Soroe Λ is too high during most of the period. There is hardly any effect of the DA system on the performance of Λ in this case, especially when considering the end of the period, though until DOY 240 the difference with the observations becomes even somewhat larger due to a small warm bias in the model. Even smaller impacts on Λ were found for other moist sites. The results are consistent with the conclusion from the sensitivity analysis that in the model context the sensitivity of Λ to soil moisture increases under dry conditions.

The surface characteristics in the model, such as LAI, albedo, roughness and water holding capacity, differ from the real surface characteristics. The possible impact of improving *LAI* on Λ is illustrated for a number of stations in Estonia, were TERRA displayed a clear seasonality in Λ. For ISBA, the seasonal change of *LAI* is much smaller in this region, while TESSEL has a constant *LAI*.

Figure 9 shows model results for the Jogeva site typical for the Estonian region. The Figure depicts the modelled 11-d moving averages of Λ, constructed from at least 6 daily values within the averaging interval. Because no flux sites are available in this area, Λ was computed using the well-known approach by Priestley and Taylor (1972), that gives reasonable estimates of λE for well-watered, dense grasslands and crops under optimal conditions. In spite of the temperature and radiation dependence, Λ from the Priestley and Taylor approach (Λ_{PT}) shows hardly any seasonal dependence. However, because the approach is developed for dense vegetation, it implicitly assumes constant *LAI*. In the next step, a dependence on *LAI* was therefore included by scaling the Priestley and Taylor λE with the *LAI* variation in the models, that is, λE was reduced by a fraction LAI/LAI_m, where LAI_m is the maximum *LAI* of the season. This is consistent with increasing

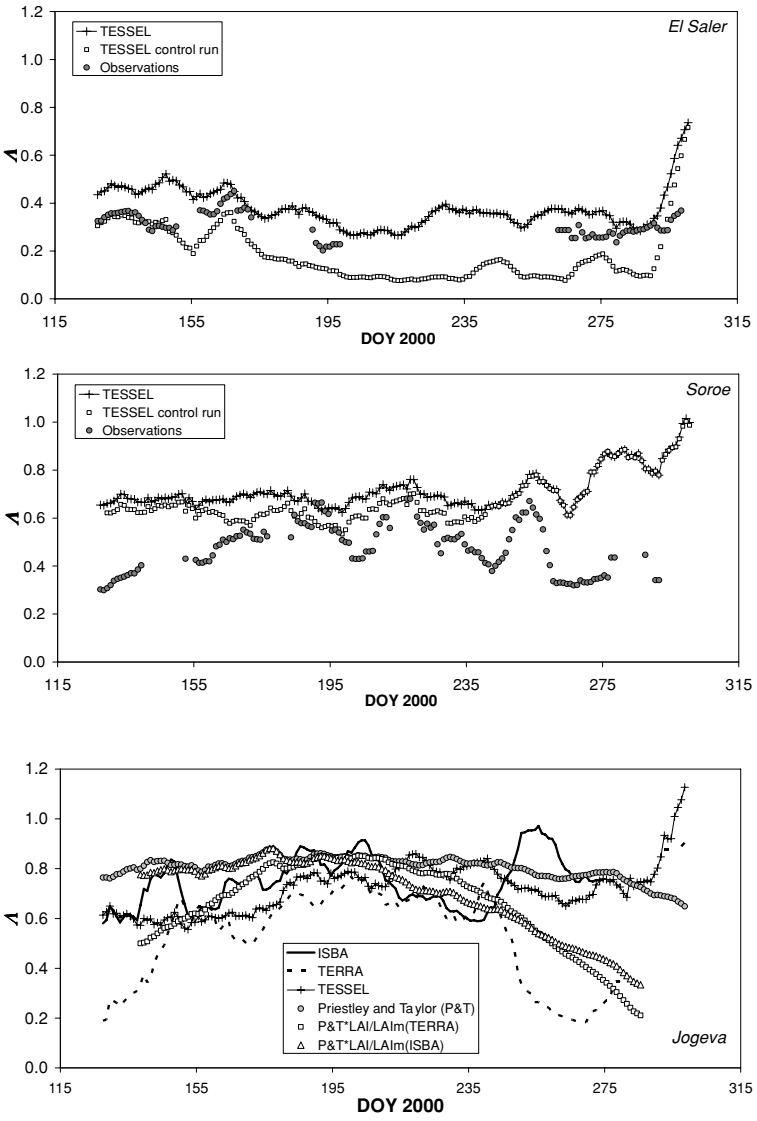

Fig. 8. Illustration of the impact of the TESSEL DA system on the evaporative fraction Λ for a typical dry and moist case, respectively. Upper panel: dry case (El Saler, Spain); Lower panel: moist case (Soroe, Denmark). Filled circles: observations; pluses TESSEL with DA system; squares: TESSEL.

Fig. 9. Illustration of the possible impact of surface properties on model output for Λ, case Jogeva, Estonia. The curves show 11-day moving averages of the evaporative fraction Λ around noon (see text). Black line: ISBA; dashed line: TERRA; pluses: TESSEL; filled circles: Λ_{PT}; triangles: Λ_{PT} multiplied by LAI/LAI$_m$ from ISBA; squares: Λ_{PT} multiplied by LAI/LAI$_m$ from TERRA.

r_s in (2), like in the models. In this way, Λ_{PT} was scaled with *LAI* from ISBA and *LAI* from TERRA, by using their monthly *LAI* values, linearly interpolated to daily *LAI* values. The results are also displayed in Fig. 9.

Accounting for the seasonal variation in *LAI* explains much of the differences between the models, especially at the start of the period investigated here. Indeed, the impact of *LAI* on Λ_{PT} was much larger than the impact of the DA system on Λ in the case of TESSEL. The 11-day moving average of Λ from the TESSEL control run for Jogeva was almost identical to the DA run and is therefore not included in Fig. 9.

5. Discussion and conclusions

In this study three LSM with land DA systems were operated and evaluated for a single growing season using in situ observations from sites spread across Europe. The systems simulate the surface energy and water balance while including a soil moisture correction term derived from errors in screen-level surface atmospheric quantities. The correction procedures are routinely applied at several NWP centres. They are designed to avoid drifts in the land surface state by correcting for random and systematic errors in the LSM forcing and model formulation. With the in situ data it is assessed whether these schemes produce adequate results regarding the annual range of the soil water content, the monthly mean soil moisture content in the root zone, and the surface evaporative fraction. Also the main reasons for differences in results produced by the various systems are explored.

By design, the configuration of the DA systems is fairly different. TERRA only used temperature as a diagnostic for deviations in soil moisture, while ISBA and TESSEL used temperature as well as relative humidity. The description of soil and vegetation

within the models was based on different databases, and the forcings were different as well. For TESSEL a single-column configuration was used, in which large-scale advection is prescribed. Also, the observation data used to evaluate the models originated from different sources, implying differences in their information content. At 24 out of 33 sites, direct soil moisture observations were available, often with very different characteristics in temporal and spatial resolution. At 14 out of the 33 sites flux observations were performed, but often no soil moisture observations were available. Also, most of the flux observations were performed over forest, and the sites tend to be located near the coast. In spite of the differences some conclusions on the functioning of the systems can be drawn.

It is shown that the systems have the tendency to damp the annual cycle of soil moisture, both immediately after precipitation events, and with respect to the seasonal time scale. This is consistent with the results of Bell et al. (2005), who found similar reductions of the amplitude in the context of a study on the effects of the DA system on river discharge. Ferranti and Viterbo (2006) argue that too wet springtime soil moisture values in the ECMWF model prevented the accurate simulation of the 2003 European heat wave.

Estimates of the monthly soil water change derived from $P–E$ measurements at a range of flux sites showed a strong reduction of the mean bias (up to a factor of 4) and a smaller RMSE improvement by applying the soil moisture correction. They do so by on average adding water to the soil during the growing season.

The mean evaporative fraction Λ (an important diagnostic for boundary layer processes and surface energy partitioning) was shown to be significantly improved under dry conditions only. The bias was on average 0.06–0.085, about 15% of the mean Λ, but displayed a seasonal cycle that was somewhat different for TERRA than for ISBA and TESSEL. The RMSE was found to range between 0.2 and 0.23 on a monthly timescale (typically $\sim$45%), and from 0.24 to 0.27 using daily noon values of Λ ($\sim$50%). The RMSE showed no consistent trend during the evaluation period.

Coming to the possible improvements to the modelling systems considered here, various options emerge. The generally larger water holding capacity of TERRA at the sites allows larger (and more realistic) seasonal soil moisture variations under otherwise similar conditions. Also, the seasonality in rooting depth and LAI in TERRA (in contrast with ISBA and TESSEL) affects E and at least partially explains the generally larger seasonal amplitude of the soil moisture simulated by this model. These characteristics can avoid a strong damping of the soil moisture seasonal cycle by the DA. However, the limited rooting depth of TERRA as compared to the other models means that this potential is used only partially.

The comparison of the soil water balance with and without the soil moisture increments revealed that for TERRA the effect of the increments was negative in the first one or two months of the simulations. This is likely related to spin-up problems in the atmosphere, giving strong precipitation bias.

The improvement of the ISBA soil moisture is mainly due to the soil moisture correction based on the precipitation bias, which often exceeded or neutralized the corrections derived from the near surface quantities. This demonstrates the importance of high-quality precipitation fields. However, precipitation forecasts in particular have proven to be difficult to improve (Ebert et al., 2003).

A theoretical sensitivity analysis of the model equations and the subsequent modelling results show a larger impact of soil moisture corrections on Λ under dry conditions than under wet conditions. A comparison between the DA system and a control simulation without DA with the TESSEL scheme confirmed that the increments are larger (and have more impact) under dry conditions. This non-linear interaction between soil and atmosphere was also noted by Ferranti and Viterbo (2006). In some occasions an overcorrection of Λ occurred. The high sensitivity of Λ to soil moisture under dry conditions warrants an adequate formulation of the soil hydraulic coefficients and root water extraction functions in the models. For example, including the ability of roots to actively deal with water shortage by increasing the capacity for water uptake (Teuling et al., 2006) would at least partially prevent Λ from dropping to low values too soon and reduce the sensitivity.

The relatively strong impact of DA on the bias, and the smaller impact on the random errors, is somewhat in contrast with the preferred role of DA in routine model correction: preferably bias-free models are used to which random corrections are applied that originate from random errors in the forcing or parametrizations. Running DA with land models that have systematic errors is difficult to avoid. In two-way coupled forecasting systems, soil moisture memorizes any error in the hydrological cycle of the models. Therefore, in forecasting mode, a need for DA will remain in order to avoid drifts of soil moisture into unrealistic states. But this introduces the risk of obscuring systematic errors in the LSM. Improvement of (land surface) models is still needed in many aspects to avoid systematic drifts or discrepancies with observations.

Model improvements should be balanced against improvements of the DA procedures per se. Our results show that ELDAS systems allow identification of systematic model errors. Once DA systems like those studied here are operational, effort should be devoted to extend the DA and to assimilate diverse observation types, for example, screen-level T and RH, microwave/infrared brightness temperatures and soil moisture products. This will then most likely result in identification of model deficiencies, as already shown by Seuffert et al. (2004) and Drusch (2007). Model bias appearing from persistent DA increments should then be addressed by model improvements, rather than left to DA systems which by definition does not deal with bias. An LSM with large systematic errors will always cause the land DA increments to tune soil moisture instead

of correcting for random errors, and will not improve physical consistency.

Analysis of persistent increments could identify areas of model improvement. For instance, it was shown here that in some occasions the soil moisture increments likely compensated for the lack of a seasonal cycle in Leaf Area Index. Under moist conditions the effect of introducing seasonality in LAI even exceeds the impact of the DA. Also, differences between the various DA systems point at the importance of using adequate soil hydraulic properties, which is another model component that may need revision. Thus, systematic evaluation of modelling systems within a DA framework using in situ data is helpful in the development of these improved modelling systems.

Because soil moisture is a crucial quantity in many models and parametrizations, direct evaluation of this quantity would be preferred. Based on the experience in the present study, we would therefore strongly support the establishment of a network of standardized and quality-controlled soil moisture observations, preferably integrated in the existing flux-observation networks such as FLUXNET (Baldocchi et al., 2001).

6. Acknowledgments

This ELDAS research has been supported by the European Commission, contract EVG1-CT-2001–00050, and by Alterra B.V., Wageningen. We would like to thank the PI's and field workers of the CarboEuroflux and BALTEX communities for making available their data. Arnold Moene and Henk de Bruin of the Meteorology and Air Quality department of Wageningen University are thanked for allowing us to use the scintillometer data. We are indebted to Finn Lars Plauborg for making available the Danish PLAP data. Finally, we thank three anonymous reviewers for their valuable comments on our manuscript.

References

Aubinet, M., Grelle, A., Ibrom, A., Rannik, U., Moncrieff, J., and co-authors. 2000. Estimates of the annual net carbon and water exchange of forests: the EUROFLUX methodology. *Adv. Ecol. Res.* **30**, 113–175.

Baldocchi, D., Falge, E., Gu, L., Olson, R., Hollinger, D., and co-authors. 2001. FLUXNET: a new tool to study the temporal and spatial variability of ecosystem-scale carbon dioxide, water vapor, and energy flux densities. *Bull. Am. Met. Soc.* **82**, 2415–2434.

Balsamo, G., Bouyssel, F. and Noilhan, J. 2004. A simplified bi-dimensional variational analysis of soil moisture from screen-level observations in a mesoscale numerical weather-prediction model. *Q. J. R. Meteorol. Soc.* **130**, 895–915.

Balsamo, G., Bouyssel, F., Noilhan, J., Mahfouf, J.-F., Bélair, S., and co-authors. 2005. A simplified variational analysis scheme for soil moisture: Developments at Météo-France and MSC. ECMWF/ELDAS workshop on Land Surface Assimilation. In: *ECMWF Proceedings. ECMWF, Reading*, UK , 79–96.

Bastiaanssen, W. G. M. 1995. Regionalization of surface flux densities and moisture indicators in composite terrain: a remote sensing approach under clear skies in Mediterranean climates. Sc-DLO, Wageningen , 273 pp.

Bell, V. A., Blyth, E. M. and Moore, R. J. 2005. The use of soil moisture in hydrological forecasting. ECMWF/ELDAS workshop on Land Surface Assimilation. In: *ECMWF Proceedings*. ECMWF, Reading, UK , 147–152.

Betts, A. K. and Viterbo, P. 2005. Land-surface, boundary layer, and cloud-field coupling over the southwestern Amazon in ERA-40. *J. Geophys. Res.* **110**, D14108, doi:10.1029/2004JD005702.

Courtier, P., Freydier, C., Geleyn, J. F., Rabier, F. and Rochas, M. 1991. The ARPEGE project at Météo-France. *Proc. ECMWF Seminar* **2**, 193–232.

Denmead, O. T. and Shaw, R. H. 1962. Availability of soil water to plants as affected by soil moisture content and meteorological conditions. *Agron. J.* **54**, 385–390.

Doms, G., Förstner, J., Heise, E., Herzog, H.-J., Raschendorfer, M., and co-authors. 2005. A description of the nonhydrostatic regional model LM, part II: physical parameterization. Available from DWD, Offenbach, and http://cosmo-model.cscs.ch/public/documentation.htm#p2, 133 pp.

Doms G. and Schättler, U. 2002. Documentation of the COSMO-model. Part I: physical parameterization. Available from DWD, Offenbach, and http://www.cosmo-model.org/content/model/documentation/core. 140 pp.

Douville, H., Viterbo, P., Mahfouf, J. F. and Beljaars, A. C. M. 2000. Evaluation of the optimum interpolation and nudging techniques for soil moisture analysis using FIFE data. *Mon. Wea. Rev.* **128**, 1733–1756.

Drusch, M. 2007. Initializing numerical weather prediction models with satellite derived surface soil moisture: data assimilation experiments with ECMWF's Integrated Forecast System. *J. Geophys. Res.* **112**, D03102, doi:10.1029/2006JD007478.

Ebert, E. E., Damrath, U., Wergen, W. and Baldwin, M. E. 2003. The WGNE assessment of short-term quantitative precipitation forecasts. *Bull. Am. Met. Soc.* **84**, 481–492.

Ek, M. B. and Holtslag, A. A. M. 2004. Influence of soil moisture on boundary layer cloud development. *J. Hydromet.* **5**, 86–99.

Ferranti, L. and Viterbo, P. 2006. The European summer of 2003: sensitivity to soil water initial conditions. *J. Climate* **19**, 3659–3680.

Hess, R. 2001. Assimilation of screen level observations by variational soil moisture analysis. *Meteorol. Atmos. Phys.* **77**, 145–154.

Hess, R., Lange, M. and Wergen, W. 2008. Evaluation of the variational soil moisture assimilation scheme at Deutscher Wetterdienst (DWD). *Q.J.R. Meteorol. Soc.* (in press).

Houser, P. R., Shuttleworth, W. J., Famiglietti, J. S., Gupta, H. V., Syed, K. H., and co-authors. 1998. Integration of soil moisture remote sensing and hydrologic modeling using data assimilation. *Water Resour. Res.* **34**, 3405–3420.

Jacobs, A. F. G., Heusinkveld, B. G., and Holtslag, A. A. M. 2008. Towards closing the surface energy budget of a mid-latitude grassland. *Boundary-Layer Meteorol.* **126**, 125–136.

Jacobs, C. M. J. and De Bruin, H. A. R. 1992. The Sensitivity of regional transpiration to land-surface characteristics – significance of feedback. *J. Climate* **5**, 683–698.

Jarvis, P. G. 1976. The interpretation of the variations in leaf water potential and stomatal conductance found in canopies in the field. *Phil. Trans. R. Soc. B* **293**, 593–610.

Jarvis, P. G. and McNaughton, K. G. 1986. Stomatal control of transpiration—scaling up from leaf to region. *Adv. Ecol. Res.* **15**, 1–49.

Lindhardt, B., Abildtrup, C., Vosgerau, H., Olsen, P., Torp, S., and co-authors. 2001. The Danish Pesticide Leaching Assessment Programme. Site Characterization and Monitoring Design. Geological Survey of Denmark and Greenland, Copenhagen , 74 pp.

Loveland, T. R., Reed, B. C., Brown, J. F., Ohlen, D. O., Zhu, Z., and co-authors. 2000. Development of a global land cover characteristics database and IGBP DISCover from 1 km AVHRR data. *Int. J. Remote Sens.* **21**, 1303–1330.

Mahfouf, J. F. 1991. Analysis of soil-moisture from near-surface parameters—a feasibility study. *J. Appl. Meteorol.* **30**, 1534–1547.

Masson, V., Champeaux, J.-L., Chauvin, F., Meriguet, C. and Lacaze, R. 2003. A global database of land surface parameters at 1-km resolution in meteorological and climate models. *J. Climate* **16**, 1261–1282.

Mauder, M., Oncley, S., Vogt, R., Weidinger, T., Ribeiro, L., and co-authors. 2007. The energy balance experiment EBEX-2000. Part II: Intercomparison of eddy-covariance sensors and post-field data processing methods. *Boundary-Layer Meteorol.* **123**, 29–54.

Meetschen, D., Van Den Hurk, B., Ament, F. and Drusch, M. 2004. Optimized surface radiation fields derived from Meteosat imagery and a regional atmospheric model. *J. Hydromet.* **5**, 1091–1101.

Meijninger, W. M. L., Green , A. E., Hartogensis, O. K., Kohsiek, W., Hoedjes, J. C. B., and co-authors. 2002. Determination of area-averaged water vapor fluxes with large aperture and radio wave scintillometers over a heterogeneous surface—flevoland field experiment. *Boundary-Layer Meteorol.* **105**, 63–83.

Moene, A. and De Bruin, H. A. R. 2001. Sensible heat flux data derived from the scintillometers. In: *Advanced Earth Observations – Land Surface Climate* (eds Z. Su and C. Jacobs). Final Report. BCRS Reports. BCRS, 85–90.

Noilhan, J. and Mahfouf, J.-F. 1996. The ISBA land surface parameterisation scheme. *Global Planet. Change* **13**, 145–159.

Oncley, S., Foken, T., Vogt, R., Kohsiek, W., DeBruin, H., and co-authors. 2007. The Energy Balance Experiment EBEX-2000. Part I: overview and energy balance. *Boundary-Layer Meteorol.* **123**, 1–28.

Priestley, C. H. B. and Taylor, R. J. 1972. On the Assessment of Surface Heat Flux and Evaporation Using Large-Scale Parameters. *Mon. Wea. Rev.* **100**, 81–92.

Raschke, E., Meywerk, J., Warrach, K., Andrea, U., Bergstrom, S., and co-authors. 2001. The Baltic Sea Experiment (BALTEX): a European contribution to the investigation of the energy and water cycle over a large drainage basin. *Bull. Am. Met. Soc.* **82**, 2389–2413.

Rhodin, A., Kucharski, F., Callies, U., Eppel, D. P. and Wergen, W. 1999. Variational analysis of effective soil moisture from screen-level atmospheric parameters: application to a short-range weather forecast model. *Q. J. R. Meteorol. Soc.* **125**, 2427–2448.

Robock, A., Schlosser, C. A., Vinnikov, K. Y., Speranskaya, N. A., Entin J. K., and co-authors. 1998. Evaluation of the AMIP soil moisture simulations. *Global Planet. Change* **19**, 181–208.

Rubel, F., Brugger, K., Skomorowski, P. and Kottek, M. 2005. Daily and 3-hourly Quantitative Precipitation Estimation for ELDAS. ECMWF/ELDAS workshop on Land Surface Assimilation. In: *ECMWF – Proceedings. ECMWF*, Reading, UK , 19–32.

Santanello, J. A., Friedl, M. A. and Kustas, W. P. 2005. An empirical investigation of convective planetary boundary layer evolution and its relationship with the land surface. *J. Appl. Meteorol.* **44**, 917–932.

Seuffert, G., Wilker, H., Viterbo, P., Drusch, M. and Mahfouf, J.-F. 2004. The usage of screen-level parameters and microwave brightness temperature for soil moisture analysis. *J. Hydromet.* **5**, 516–531.

Teuling, A. J., Uijlenhoet, R., Hupet, F. and Troch, P. A. 2006. Impact of plant water uptake strategy on soil moisture and evapotranspiration dynamics during drydown. *Geophys. Res. Lett.* **33**, L03401, doi:03410.01029/02005GL025019.

Uppala, S. M., Kallberg, P. W., Simmons, A. J., Andrae, U., Bechtold, V. D., and co-authors. 2005. The ERA-40 re-analysis. *Q. J. R. Meteorol. Soc.* **131**, 2961–3012.

Valentini, R., Matteucci, G., Dolman, A. J., Schulze, E. D., Rebmann, C., and co-authors, 2000. Respiration as the main determinant of carbon balance in European forests. *Nature* **404**, 861–865.

Van Den Hurk, B. J. J. M. 2002. European LDAS established. *Gewex Newslett.* **12**, 9.

Van Den Hurk, B. J. J. M., Bastiaanssen, W. G. M., Pelgrum, H. and Van Meijgaard, E. 1997. A new methodology for assimilation of initial soil moisture fields in weather prediction models using Meteosat and NOAA data. *J. Appl. Meteorol.* **36**, 1271–1283.

Van Den Hurk, B. J. J. M., Ettema J. and Viterbo, P., 2008. Analysis of soil moisture changes in Europe during a single growing season in a new ECMWF soil moisture assimilation system. *J. Hydromet.* **9**, 116–131.

Van Den Hurk, B. J. J. M., Viterbo, P., Beljaars, A. C. M. and Betts, A. K. 2000. Offline validation of the ERA40 surface scheme. In: *Technical Memorandum 295, European Centre for Medium-Range Weather Forecasts*, Reading.

Viterbo, P. 1996. The representation of surface processes in general circulation models. In: *ECMWF*, Reading, UK , 201 pp.

Viterbo, P. and Beljaars, A. C. M. 1995. An improved land surface parameterization scheme in the ECMWF model and its validation. *J. Climate* **8**, 2716–2748.

Wergen, W., Hess, R. and Lange, M. 2005. Variational soil assimilation at DWD. In: *ECMWF/ELDAS workshop on Land Surface Assimilation. ECMWF – Proceedings. ECMWF*, Reading, UK , 69–77.